

# LaSr<sub>3</sub>Fe<sub>3-y</sub>Co<sub>y</sub>O<sub>10-δ</sub> (0 ≤ y ≤ 1.5) Intergrowth Oxide Cathodes for Intermediate Temperature Solid Oxide Fuel Cells

K. T. Lee and A. Manthiram\*

Materials Science and Engineering Program, University of Texas at Austin, Austin, Texas 78712

Received November 30, 2005. Revised Manuscript Received January 26, 2006

LaSr<sub>3</sub>Fe<sub>3-y</sub>Co<sub>y</sub>O<sub>10-δ</sub> (0 ≤ y ≤ 1.5) oxides with a perovskite-related intergrowth structure have been investigated as cathode materials for oxygen reduction reaction in intermediate temperature solid oxide fuel cells (SOFC). The electrical conductivity, oxygen vacancy concentration, and thermal expansion coefficient (TEC) increase with increasing Co content y. The electrocatalytic activity and power density measured with the LaSr<sub>3</sub>Fe<sub>3-y</sub>Co<sub>y</sub>O<sub>10-δ</sub>/La<sub>0.8</sub>Sr<sub>0.2</sub>Ga<sub>0.8</sub>Mg<sub>0.2</sub>O<sub>2.8</sub> (LSGM)/Ni–Ce<sub>0.9</sub>Gd<sub>0.1</sub>O<sub>1.95</sub> (GDC) single cells with a porous Ce<sub>0.9</sub>Gd<sub>0.1</sub>O<sub>1.95</sub> (GDC) interlayer between the cathode and the electrolyte to avoid undesired interfacial reactions increase with increasing Co content because of an increase in the electronic and oxide ion conductivities of the cathode. The intergrowth LaSr<sub>3</sub>Fe<sub>3-y</sub>Co<sub>y</sub>O<sub>10-δ</sub> cathodes offer electrochemical performances comparable to that of the well-known perovskite La<sub>0.6</sub>Sr<sub>0.4</sub>CoO<sub>3-δ</sub> cathode but with an important advantage of significantly lower TEC.

## 1. Introduction

Solid oxide fuel cells (SOFC) offer an important advantage of directly using the hydrocarbon fuels such as natural gas without requiring external fuel reforming to produce hydrogen, but they suffer from high chemical reactivity and thermal expansion mismatch among the components at the conventional operating temperature of >900 °C. These difficulties have generated interest in recent years to lower the operating temperatures to an intermediate level of 500–800 °C. However, one of the major issues with the intermediate temperature SOFC is the slow kinetics of the oxygen reduction reaction and the consequent high overpotential at the cathode. Although conventional SOFC technology operating at >900 °C uses the La<sub>1-x</sub>Sr<sub>x</sub>MnO<sub>3</sub> perovskite as the cathode, its catalytic activity for the oxygen reduction reaction is inadequate at <800 °C.<sup>1</sup> Moreover, the stability of the Mn<sup>4+</sup> oxidation state at elevated temperatures results in little or no oxide ion vacancies in La<sub>1-x</sub>Sr<sub>x</sub>MnO<sub>3</sub>. Consequently, it is not an oxide ion conductor, which limits the location of the oxygen reduction reaction to an electrolyte–electrode–O<sub>2</sub> triple phase boundary (TPB). In contrast, the cobalt-containing perovskite oxides such as La<sub>1-x</sub>Sr<sub>x</sub>CoO<sub>3-δ</sub> sustain significant amount of oxide ion vacancies because of the lower stability of the Co<sup>4+</sup> oxidation state and exhibit high oxide ion conductivity with lower overpotentials.<sup>2</sup> Unfortunately, oxides with significant amounts of Co exhibit large thermal expansion because of the spin state transitions associated with the Co<sup>3+</sup> ion and the high chemical reactivity with the electrolyte.<sup>3</sup>

ABO<sub>3-δ</sub> perovskite oxides are the most widely investigated mixed ionic-electronic conductors and cathodes for SOFC

in the literature. More recently, perovskite-related intergrowth oxides<sup>4–6</sup> A<sub>n+1</sub>B<sub>n</sub>O<sub>3n+1</sub> (A = lanthanide or alkaline earth, B = transition metal, and n = 1–3) belonging to the Ruddlesden–Popper series have drawn some attention as mixed conductors.<sup>4–9</sup> These intergrowth oxides have structures in which the (AO)<sub>2</sub> double rock-salt layers alternate with the A<sub>n-1</sub>B<sub>n</sub>O<sub>3n-1</sub> perovskite layers along the c axis, giving a two-dimensional structure.<sup>10</sup> We have shown that the intergrowth oxides Sr<sub>3-x</sub>La<sub>x</sub>Fe<sub>2-y</sub>Co<sub>y</sub>O<sub>7-δ</sub> with 0 ≤ x ≤ 0.3 and 0 ≤ y ≤ 1.0 (n = two member) and LaSr<sub>3</sub>Fe<sub>3-y</sub>Co<sub>y</sub>O<sub>10-δ</sub> with 0 ≤ y ≤ 1.5 (n = three member) exhibit good mixed ionic-electronic conduction with adequate oxide ion and electronic conductivities and are attractive as oxygen separation membranes.<sup>6–9</sup> More importantly, these oxides exhibit excellent structural stability with no crystallographic phase transformations up to 900 °C even under low pO<sub>2</sub> conditions, unlike most of the Co- and Fe-containing ABO<sub>3-δ</sub> perovskite oxides, suggesting good long-term stability for the intergrowth oxides.

However, the A<sub>n+1</sub>B<sub>n</sub>O<sub>3n+1</sub> intergrowth oxides have not been explored as cathodes for SOFC, excepting the n = one-member La<sub>2</sub>NiO<sub>4+δ</sub><sup>4,5</sup> that contains δ excess oxide ions located at the tetrahedral interstitial sites of the (LaO)<sub>2</sub> double rock-salt layers. La<sub>2</sub>NiO<sub>4+δ</sub> exhibits rather low electronic conductivity because of the Ni<sup>2+/3+</sup> couple. In contrast, the n = two and three members with the Fe<sup>3+/4+</sup> and Co<sup>3+/4+</sup> couples offer much higher electronic conductivity because of an increased O–B–O interaction along the c axis and a

(4) Skinner, S. J.; Kilner, J. A. *Solid State Ionics* **2000**, *135*, 709.

(5) Kilner, J. A.; Shaw, C. K. M. *Solid State Ionics* **2002**, *154*, 523.

(6) Prado, F.; Armstrong, T.; Caneiro, A.; Manthiram, A. *J. Electrochem. Soc.* **2001**, *148*, 37.

(7) Prado, F.; Manthiram, A. *J. Solid State Chem.* **2001**, *158*, 307.

(8) Armstrong, T.; Prado, F.; Manthiram, A. *Solid State Ionics* **2001**, *140*, 89.

(9) Manthiram, A.; Prado, F.; Armstrong, T. *Solid State Ionics* **2002**, *152*, 647.

(10) Ruddlesden, S. N.; Popper, P. *Acta Crystallogr.* **1958**, *11*, 54.

\* To whom correspondence should be addressed. Phone: +1 512 471 1791; fax: +1 512 471 7681; e-mail: rmanth@mail.utexas.edu.

(1) Jiang, S. P. *J. Power Sources* **2003**, *124*, 390.

(2) Petrov, A. N.; Kononchuk, O. F.; Andreev, A. V.; Cherepano, V. A.; Kofstad, P. *Solid State Ionics* **1995**, *80*, 189.

(3) Minh, N. Q. *J. Am. Ceram. Soc.* **1993**, *76*, 563.

smaller charge-transfer gap between the  $\text{Fe}^{3+/4+}3d$  or  $\text{Co}^{3+/4+}3d$  band and the  $\text{O}^{2-}2p$  band.<sup>6–9</sup> With this perspective, we present here the characterization of  $\text{LaSr}_3\text{Fe}_{3-y}\text{Co}_y\text{O}_{10-\delta}$  ( $0 \leq y \leq 1.5$ ) as cathode materials for intermediate temperature SOFC. The effect of Co content on the electrical conductivity, thermal expansion, chemical compatibility, and electrochemical performance is presented. We also show the effect of  $\text{Ce}_{0.9}\text{Gd}_{0.1}\text{O}_{1.95}$  (GDC) interlayer in preventing undesirable reactions between the cathode and the electrolyte.

## 2. Experimental Section

The  $\text{LaSr}_3\text{Fe}_{3-y}\text{Co}_y\text{O}_{10-\delta}$  ( $0 \leq y \leq 1.5$ ) samples were synthesized by solid-state reaction. Required amounts of  $\text{La}_2\text{O}_3$ ,  $\text{SrCO}_3$ ,  $\text{Fe}_2\text{O}_3$ , and  $\text{Co}_3\text{O}_4$  were first calcined at  $1000^\circ\text{C}$  for 12 h, were ground, and finally were fired at  $1400^\circ\text{C}$  for 24 h. The  $\text{La}_{0.8}\text{Sr}_{0.2}\text{Ga}_{0.8}\text{Mg}_{0.2}\text{O}_{2.8}$  (LSGM) electrolyte was prepared by firing required amounts of  $\text{La}_2\text{O}_3$ ,  $\text{SrCO}_3$ ,  $\text{Ga}_2\text{O}_3$ , and  $\text{MgO}$  at  $1100^\circ\text{C}$  for 5 h, followed by pelletizing and sintering at  $1500^\circ\text{C}$  for 10 h. NiO– $\text{Ce}_{0.9}\text{Gd}_{0.1}\text{O}_{1.95}$  (GDC) cermet (Ni:GDC = 70:30 vol %) anode was synthesized by the glycine–nitrate combustion method.<sup>11</sup>

Thermal expansion coefficients (TECs) of the sintered samples were measured by a Perkin-Elmer series 7 thermal analysis system from room temperature to  $700^\circ\text{C}$  with a heating/cooling rate of  $10^\circ\text{C}/\text{min}$ . Electrical conductivity was measured by a four-probe dc method in the temperature range of  $200$ – $900^\circ\text{C}$ . All the samples used for conductivity and thermal expansion measurements had densities of  $>95\%$  of the theoretical values.

Electrochemical performances were evaluated by single cell test and ac impedance analysis. The  $\text{LaSr}_3\text{Fe}_{3-y}\text{Co}_y\text{O}_{10-\delta}$  cathodes and NiO-GDC cermet anode were prepared by screen printing the slurries prepared with the sample powder and an organic binder (Heraeus V006) onto a 0.7-mm-thick LSGM electrolyte pellet followed by firing for 3 h at  $950^\circ\text{C}$  for the cathode and  $1200^\circ\text{C}$  for the anode. For the  $\text{LaSr}_3\text{Fe}_{3-y}\text{Co}_y\text{O}_{10-\delta}$  cathodes with the GDC interlayer, both the cathode and the interlayer were first prepared by screen printing and then were cofired at  $1100^\circ\text{C}$  for 3 h. For a comparison, the electrochemical performance was also evaluated with the  $\text{La}_{0.6}\text{Sr}_{0.4}\text{CoO}_{3-\delta}$  (LSC) perovskite cathode that was synthesized by a solid-state reaction at  $1200^\circ\text{C}$  for 24 h and was fired after screen printing at  $1000^\circ\text{C}$  for 3 h. The geometrical area of all the electrodes was  $0.25\text{ cm}^2$ .  $I$ – $V$  measurements of single cells were carried out at  $800^\circ\text{C}$  with a three-electrode configuration, which allows for separating and monitoring cathode overpotentials during the cell operation. Pt paste was used as the reference electrode. The detailed single cell configuration has been described elsewhere.<sup>12</sup> Humidified  $\text{H}_2$  ( $\sim 3\% \text{ H}_2\text{O}$  at  $30^\circ\text{C}$ ) and air were supplied as fuel and oxidant, respectively, at a rate of  $100\text{ cm}^3/\text{min}$ . ac impedance was measured in air by a potentiostat with a three-electrode configuration, and the test cell geometry and configuration were the same as that used for the single cell performance test. Pt paste was used as both the counter and the reference electrodes, and the applied frequency was in the range of  $0.5\text{ mHz}$  to  $1\text{ MHz}$  with the voltage amplitude of  $10\text{ mV}$ .

## 3. Results and Discussion

The temperature dependence of the electrical conductivity of the  $\text{LaSr}_3\text{Fe}_{3-y}\text{Co}_y\text{O}_{10-\delta}$  samples is shown in Figure 1. All the samples exhibit a thermally activated semiconducting

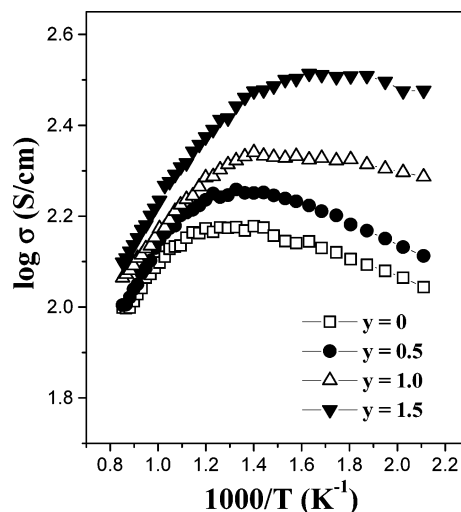


**Figure 1.** Variations of the electrical conductivity of  $\text{LaSr}_3\text{Fe}_{3-y}\text{Co}_y\text{O}_{10-\delta}$  ( $0 \leq y \leq 1.5$ ) with temperature in air.

behavior at lower temperatures ( $<400^\circ\text{C}$ ), with the conductivity increasing with increasing temperature. However, the conductivity decreases with increasing temperature above a transition temperature  $T_t$  of about  $300$ – $500^\circ\text{C}$  because of a significant loss of oxygen from the lattice as indicated by the TGA data.<sup>8</sup> The formation of oxide ion vacancies accompanied by a reduction of  $\text{Fe}^{4+}$  to  $\text{Fe}^{3+}$  or  $\text{Co}^{4+}$  to  $\text{Co}^{3+}$  at higher temperatures causes a decrease in the charge carrier concentration and covalent interaction because of a perturbation of the O–(Fe,Co)–O periodic potential,<sup>12,13</sup> resulting in a decrease in conductivity. The transition temperature  $T_t$  decreases slightly with increasing Co content  $y$  because of a lowering of the temperature at which oxygen loss begins to occur in air with increasing Co content.<sup>8</sup> At a given temperature, the electrical conductivity increases monotonically with increasing Co content because of an increase in the covalency of the (Co–Fe)–O bond. Matsumoto et al.<sup>14</sup> and Dasgupta et al.<sup>15</sup> have also reported a similar trend, respectively, for the perovskite systems  $\text{La}_{1-x}\text{Sr}_x\text{Fe}_{1-y}\text{Co}_y\text{O}_3$  and  $\text{Nd}_{0.7}\text{Sr}_{0.3}\text{Fe}_{1-x}\text{Co}_x\text{O}_3$ .

The thermal expansion behaviors of the  $\text{LaSr}_3\text{Fe}_{3-y}\text{Co}_y\text{O}_{10-\delta}$  samples at  $50$ – $700^\circ\text{C}$  in air are shown in Figure 2a. The nonlinear thermal expansion curve could be fitted with a fourth polynomial regression,<sup>16</sup> and the average TEC values obtained with the fitting are plotted as a function of Co content in Figure 2b. The TEC value increases with increasing Co content. The  $\text{Co}^{3+}$  ions experience a low spin ( $t_{2g}^6e_g^0$ ) to high spin ( $t_{2g}^4e_g^2$ ) transition as the temperature increases.<sup>17,18</sup> Considering the larger ionic radius of the high spin  $\text{Co}^{3+}$  ion ( $r = 0.61\text{ \AA}$ ) compared to that of the low spin  $\text{Co}^{3+}$  ion ( $r = 0.545\text{ \AA}$ ), the spin state transition leads to a

(11) Chick, L. A.; Pedersen, L. R.; Maupin, G. D.; Bates, J. L.; Thomas, L. E.; Exarhos, G. J. *Mater. Lett.* **1990**, *10*, 6.  
 (12) Lee, K. T.; Manthiram, A. *J. Power Sources*, in press.

(13) Takahashi, H.; Munakata, F.; Yamanaka, M. *Phys. Rev. B* **1998**, *57*, 15211.

(14) Matsumoto, Y.; Yamamoto, S.; Nishida, T.; Sato, E. *J. Electrochem. Soc.* **1980**, *27*, 2360.

(15) Dasgupta, N.; Krishnamoorthy, R.; Jacob, K. T. *Mater. Sci. Eng., B* **2002**, *90*, 278.

(16) Chavan, S. V.; Patwe, S. J.; Tyagi, A. K. *J. Alloys Compd.* **2003**, *360*, 189.

(17) Raccach, P. M.; Goodenough, J. B. *Phys. Rev.* **1967**, *155*, 932.

(18) Bhide, V. G.; Rajoria, D. S.; Reddy, Y. S.; Rama Rao, G.; Subba Rao, G. V.; Rao, C. N. R. *Phys. Rev. Lett.* **1972**, *28*, 1133.

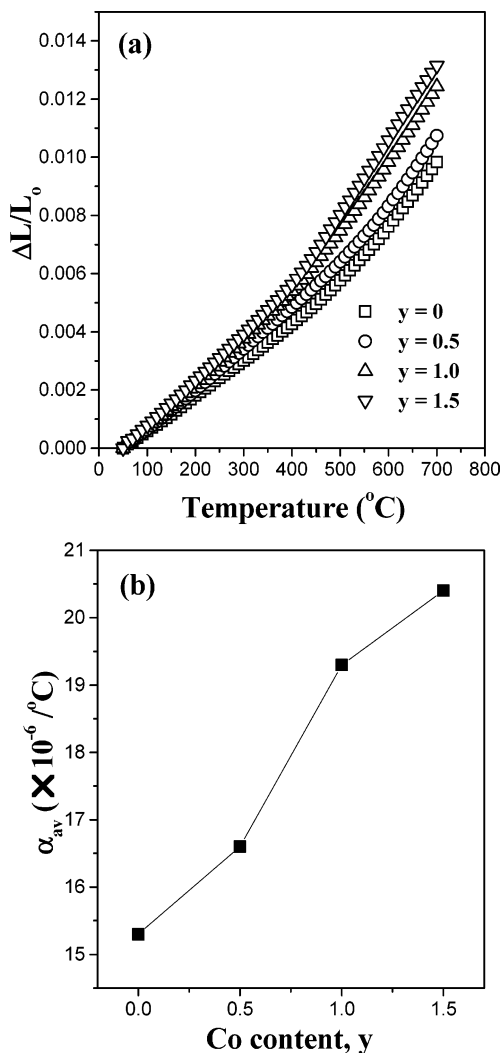


**Figure 2.** Thermal expansion behaviors of  $\text{LaSr}_3\text{Fe}_{3-y}\text{Co}_y\text{O}_{10-\delta}$  ( $0 \leq y \leq 1.5$ ) in air: (a) thermal expansion ( $\Delta L/L_0$ ) curves with temperature and (b) average thermal expansion coefficients ( $\alpha_{av}$ ) with Co content  $y$  in the temperature range of 50–700  $^{\circ}\text{C}$ .

larger TEC for the Co-based perovskite systems.<sup>19,20</sup> Therefore, the spin state transitions associated with the  $\text{Co}^{3+}$  ions within the perovskite blocks of the present intergrowth oxide system could contribute to the increase in TEC with Co doping. TEC can also increase with increasing oxide ion vacancies because of a reduction in the electrostatic attractive forces between the cations and anions<sup>21,22</sup> and a reduction of the smaller  $\text{Fe}^{4+}$  or  $\text{Co}^{4+}$  to larger  $\text{Fe}^{3+}$  or  $\text{Co}^{3+}$  ions. Since the degree of oxygen loss increases with Co content in  $\text{LaSr}_3\text{Fe}_{3-y}\text{Co}_y\text{O}_{10-\delta}$ ,<sup>8</sup> it could also contribute to the increase in TEC with Co content. The temperature at which the expansion curve deviates from linearity decreases slightly with increasing Co content, which attests to the influence of the formation of oxide ion vacancies on the lattice expansion. Furthermore, TEC is inversely proportional to the bonding energy between the ions in the lattice.<sup>23</sup> A lower standard

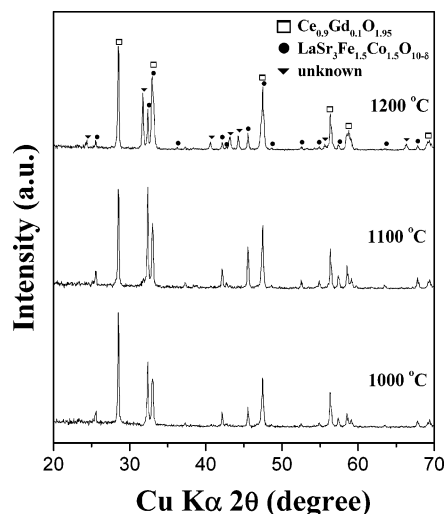


**Figure 3.** X-ray power diffraction patterns of  $\text{LaSr}_3\text{Fe}_{1.5}\text{Co}_{1.5}\text{O}_{10-\delta}$  and GDC mixture after firing at various temperatures for 3 h in air.

Gibbs free energy of formation for  $\text{Co}_3\text{O}_4$  (−794.871 kJ/mol) compared to that for  $\text{Fe}_3\text{O}_4$  (−1017.438 kJ/mol)<sup>24</sup> implies that the Co–O bond is weaker than the Fe–O bond. Thus, the decrease in bonding energy with Co doping could also cause an increase in TEC.

One issue with the perovskite-related intergrowth oxide cathodes is the interfacial reaction with the yttria-stabilized zirconia (YSZ) or the LSGM electrolytes. The  $\text{LaSr}_3\text{Fe}_{3-y}\text{Co}_y\text{O}_{10-\delta}$  samples react with LSGM at 1000  $^{\circ}\text{C}$  and form undesired reaction products. This reaction problem could be overcome by adopting an interlayer between the cathode and the electrolyte, and there is some knowledge of the  $\text{CeO}_2$ -based interlayers on the YSZ electrolyte.<sup>25–28</sup> The interlayer or the buffer layer should not react with both the cathode and the electrolyte and should have high oxide ion conductivity to enhance the oxide ion diffusion. Figure 3 shows the X-ray diffraction patterns of the  $\text{LaSr}_3\text{Fe}_{1.5}\text{Co}_{1.5}\text{O}_{10-\delta}$  and GDC ( $\text{Ce}_{0.9}\text{Gd}_{0.1}\text{O}_{1.95}$ ) mixtures after heat treatment at various temperatures. While the samples fired at 1000 and 1100  $^{\circ}\text{C}$  show no interfacial reaction, reflections corresponding to unknown reaction products are found on firing at 1200  $^{\circ}\text{C}$ . The compositions with lower Co contents also do not react with GDC at 1100  $^{\circ}\text{C}$  (Figure 4). This indicates that the intergrowth oxide cathodes could be fired at least at 1100  $^{\circ}\text{C}$  to get good adhesion without the undesired interfacial reaction. Similarly, no reaction product was detected after firing GDC and LSGM at 1200  $^{\circ}\text{C}$  for 3 h. However, although X-ray diffraction does not indicate the formation of new phases, diffusion of ionic species across the interface between different phases could not be completely ruled out.

(19) Huang, K.; Lee, H. Y.; Goodenough, J. B. *J. Electrochem. Soc.* **1998**, *145*, 3220.

(20) Mori, M.; Sammes, N. M. *Solid State Ionics* **2000**, *146*, 301.

(21) Hayashi, H.; Kanoh, M.; Quan, C. J.; Inaba, H.; Wang, S.; Dokiya, M.; Tagawa, H. *Solid State Ionics* **2000**, *132*, 227.

(22) Ullmann, H.; Trofimenko, N.; Tietz, F.; Stöver, D.; Ahmad-Khanlou, A. *Solid State Ionics* **2000**, *138*, 79.

(23) Ruffa, A. R. *J. Mater. Sci.* **1980**, *15*, 2258.

(24) Chase, M. W., Jr.; Davies, C. A.; Downey, J. R., Jr.; Frurip, D. J.; McDonald, R. A.; Syverud, N. *J. Phys. Chem. Ref. Data* **1985**, *118*, 926.

(25) Uchida, H.; Arisaka, S.; Watanabe, M. *Electrochem. Solid-State Lett.* **1999**, *2*, 428.

(26) Simmer, S. P.; Bonnett, J. F.; Canfield, N. L.; Meinhardt, K. D.; Shelton, J. P.; Sprengle, V. L.; Stevenson, J. W. *J. Power Sources* **2003**, *113*, 1.

(27) Nguyen, T. L.; Kobayashi, K.; Honda, T.; Iimura, Y.; Kato, K.; Negishi, A.; Nozaki, K.; Tappero, F.; Sasaki, K.; Shirahama, H.; Ota, K.; Dokiya, M.; Kato, T. *Solid State Ionics* **2004**, *174*, 163.

(28) Mai, A.; Haanappel, V. A. C.; Uhlenbruck, S.; Tietz, R.; Stöver, D. *Solid State Ionics* **2005**, *176*, 1341.

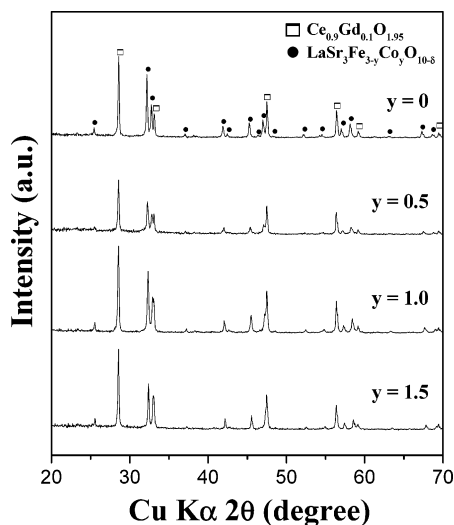


**Figure 4.** X-ray power diffraction patterns of  $\text{LaSr}_3\text{Fe}_{3-y}\text{Co}_y\text{O}_{10-d}$  ( $0 \leq y \leq 1.5$ ) and GDC mixture after firing at 1100 °C for 3 h in air.

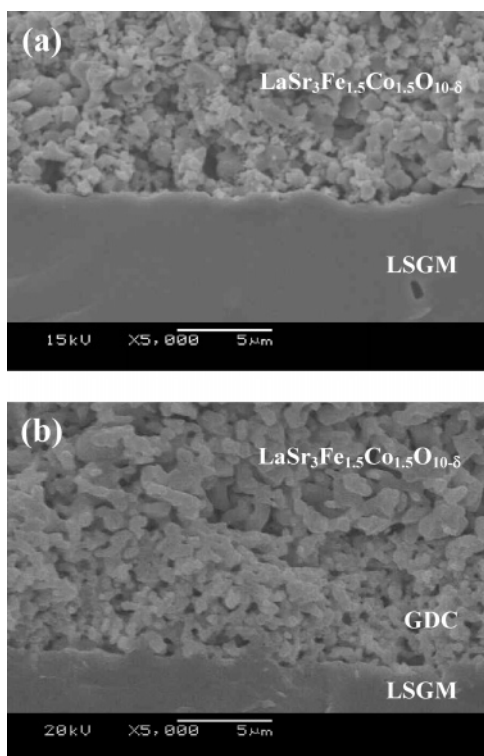


**Figure 5.** SEM micrographs of the  $\text{LaSr}_3\text{Fe}_{1.5}\text{Co}_{1.5}\text{O}_{10-d}$  cathodes that were prepared (a) without and (b) with the GDC interlayer by firing, respectively, at 950 and 1100 °C for 3 h

The firing temperature of the cathode could also affect the microstructure and consequently the electrochemical performance. Figure 5 shows the typical SEM micrographs of the cross section of the porous  $\text{LaSr}_3\text{Fe}_{1.5}\text{Co}_{1.5}\text{O}_{10-d}$  cathodes without and with the GDC interlayer on the LSGM electrolyte after firing, respectively, at 950 and 1100 °C for 3 h. Without the GDC interlayer, the  $\text{LaSr}_3\text{Fe}_{1.5}\text{Co}_{1.5}\text{O}_{10-d}$  cathode should be fired below 1000 °C to avoid the interfacial reaction. As seen in Figure 5, the  $\text{LaSr}_3\text{Fe}_{1.5}\text{Co}_{1.5}\text{O}_{10-d}$  cathode without the GDC interlayer fired at 950 °C has only point contacts between particles and poor adhesion between the cathode and electrolyte because of low firing temperature. On the other hand, the  $\text{LaSr}_3\text{Fe}_{1.5}\text{Co}_{1.5}\text{O}_{10-d}$  cathode with the GDC interlayer fired at 1100 °C shows area

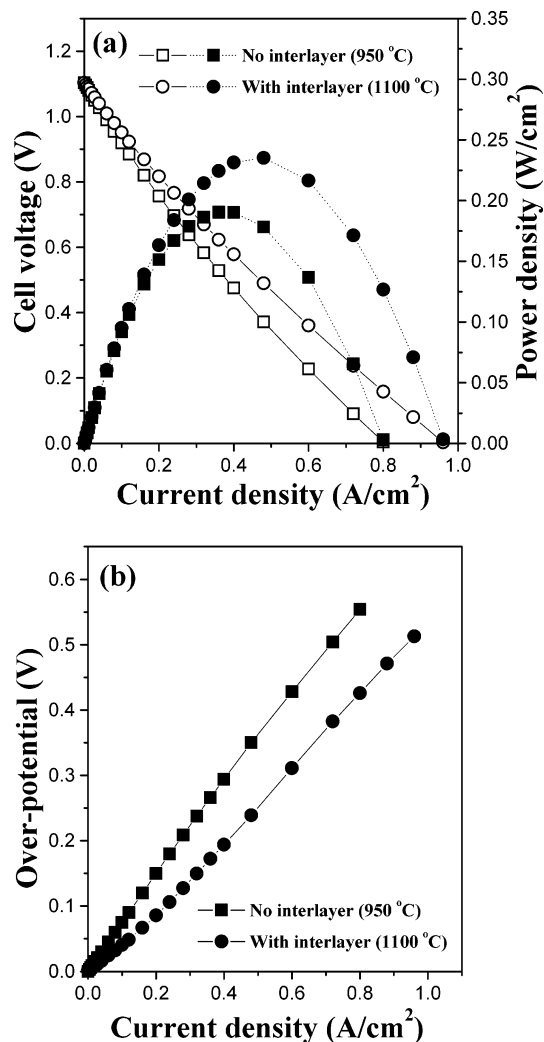


**Figure 6.** Comparison of (a) the  $I$ - $V$  curves (open symbols) and power densities (closed symbols) and (b) cathode overpotentials of the  $\text{LaSr}_3\text{Fe}_{1.5}\text{Co}_{1.5}\text{O}_{10-d}$  cathodes with and without the GDC interlayer at 800 °C. The temperatures in the legend refer to the cofiring temperatures.

contacts between particles and good adhesion between each layer. The smaller grain size of the GDC interlayer compared to that of the  $\text{LaSr}_3\text{Fe}_{1.5}\text{Co}_{1.5}\text{O}_{10-d}$  layer is due to the poor sinterability of the GDC particles. In addition to preventing the interfacial reaction, the GDC layer should be sufficiently dense to maximize the oxide ion transport since it is an extension of the electrolyte as an oxide ion conductor. Therefore, further studies to improve the sinterability of the GDC interlayer could prove beneficial.

The electrochemical performances of the  $\text{LaSr}_3\text{Fe}_{3-y}\text{Co}_y\text{O}_{10-d}$  cathodes were evaluated with an electrolyte-supported single cell fabricated with the LSGM electrolyte and GDC-Ni (30:70 vol %) anode. Figure 6 compares the  $I$ - $V$  curves, the power density, and the overpotential of the  $\text{LaSr}_3\text{Fe}_{1.5}\text{Co}_{1.5}\text{O}_{10-d}$  cathodes with and without the GDC interlayer at 800 °C. The  $\text{LaSr}_3\text{Fe}_{1.5}\text{Co}_{1.5}\text{O}_{10-d}$  cathode with the GDC interlayer exhibits a lower overpotential and a higher maximum power density than that without the GDC interlayer. This indicates that the  $\text{LaSr}_3\text{Fe}_{1.5}\text{Co}_{1.5}\text{O}_{10-d}$  cathode with the GDC interlayer exhibits good catalytic activity and the GDC interlayer does not sacrifice the catalytic activity.

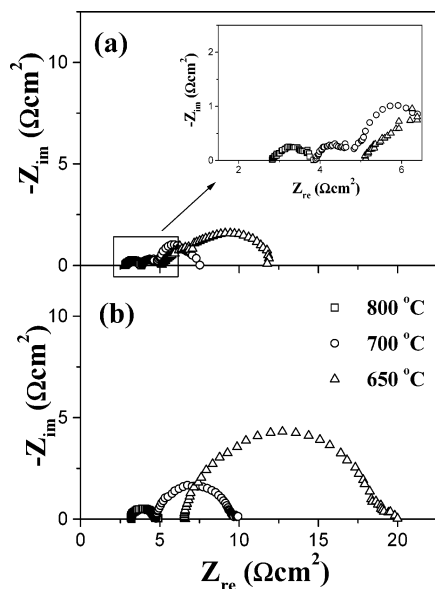


**Figure 7.** Typical ac impedance spectra of the  $\text{LaSr}_3\text{Fe}_{1.5}\text{Co}_{1.5}\text{O}_{10-\delta}$  cathodes (a) with and (b) without the GDC interlayer at various temperatures in air. The inset in (a) shows an expansion of the high-frequency region.

The ac impedance spectra of the  $\text{LaSr}_3\text{Fe}_{1.5}\text{Co}_{1.5}\text{O}_{10-\delta}$  cathodes with and without the GDC interlayer at various temperatures in air are shown in Figure 7. At all temperatures, the  $\text{LaSr}_3\text{Fe}_{1.5}\text{Co}_{1.5}\text{O}_{10-\delta}$  cathode with GDC interlayer shows lower total resistance  $R_{\text{tot}}$  (right intercept on  $Z_{\text{re}}$  axis) than that without the GDC interlayer. The temperature dependences of the ohmic resistance  $R_b$  (left intercept on  $Z_{\text{re}}$  axis) and polarization resistance  $R_p$  ( $R_{\text{tot}} - R_b$ ) are shown in Figure 8. Although GDC has much higher resistivity than  $\text{LaSr}_3\text{Fe}_{1.5}\text{Co}_{1.5}\text{O}_{10-\delta}$ , the cathode with the GDC interlayer shows lower ohmic resistance than that without the GDC interlayer (Figure 8a). As seen in Figure 5, the  $\text{LaSr}_3\text{Fe}_{1.5}\text{Co}_{1.5}\text{O}_{10-\delta}$  cathode with the GDC interlayer fired at 1100 °C for 3 h has good area contact between particles with good adhesion between the cathode and electrolyte layers, which leads to lower contact and ohmic resistances. Large enough area contact and good adhesion can not only decrease the contact resistance but also improve the electron motion and oxide ion diffusion, resulting in decreased polarization resistance as shown in Figure 8b. It is possible that the GDC interlayer may also offer some catalytic activity for the oxygen reduction reaction as has been reported by others.<sup>25–27,29</sup> Thus, the better single cell performance of the  $\text{LaSr}_3\text{Fe}_{1.5}\text{Co}_{1.5}\text{O}_{10-\delta}$  cathode with the GDC interlayer (Figure 6) is due to a reduction in not only the ohmic loss but also in the polarization loss.

The variations of the  $I$ – $V$  curve, power density, and overpotential at 800 °C for the various  $\text{LaSr}_3\text{Fe}_{3-y}\text{Co}_y\text{O}_{10-\delta}$  cathode compositions with the GDC interlayer are shown in Figure 9. For a comparison, the data for the perovskite  $\text{La}_{0.6}\text{Sr}_{0.4}\text{CoO}_{3-\delta}$  (LSC) cathode with the GDC interlayer under similar experimental conditions are also shown in Figure 9. The power density increases and the overpotential decreases with increasing Co content for the intergrowth  $\text{LaSr}_3\text{Fe}_{3-y}\text{Co}_y\text{O}_{10-\delta}$  cathodes. For all the compositions

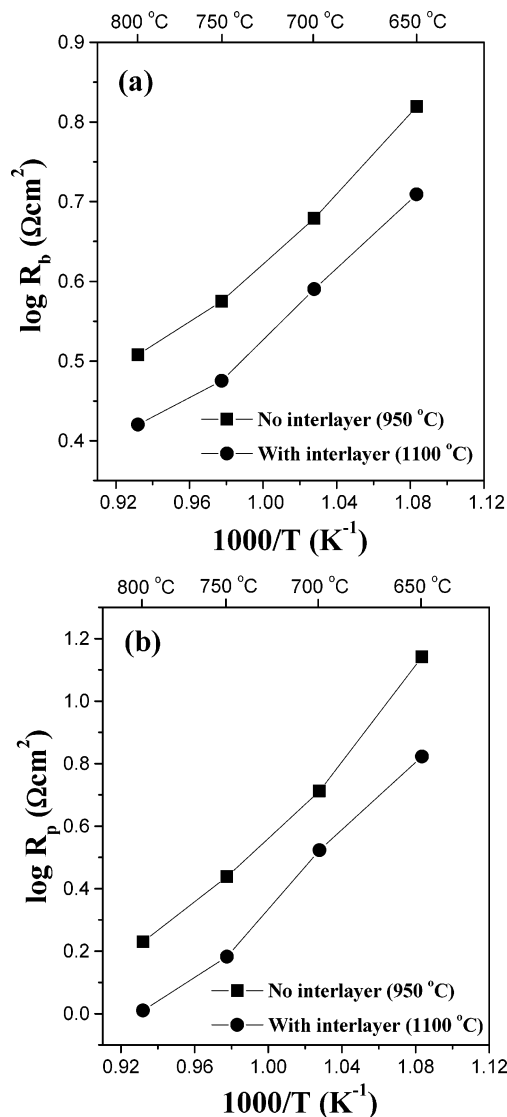


**Figure 8.** Temperature dependence of (a) ohmic ( $R_b$ ) and (b) polarization ( $R_p$ ) resistances of the  $\text{LaSr}_3\text{Fe}_{1.5}\text{Co}_{1.5}\text{O}_{10-\delta}$  cathodes with and without the GDC interlayer. The results were derived from the ac impedance data. The temperatures in the legend refer to the cofiring temperatures.

investigated, the electrochemical performance was stable without any significant degradation during the test period. Since the oxygen reduction reaction is considered as a multiphase catalytic reaction, the oxide ion mobility and surface exchange (the adsorption/dissociation of oxygen molecule) as well as the electronic conductivity of the cathode material are critical to maximize the electrochemical performance. The electrical conductivity increases with increasing Co content (Figure 1), and the substitution of  $\text{Co}^{3+}$  for  $\text{Fe}^{3+}$  increases the concentration of the oxide ion vacancies as indicated by the TGA data.<sup>8</sup> The oxygen permeability, which is controlled by the transport or mobility of oxide ions, also increases with increasing Co content.<sup>8</sup> The surface oxygen exchange coefficient is directly proportional to the mobile fraction of the oxide ion vacancies.<sup>30</sup> Gao et al.<sup>31</sup> have also reported that high oxide ion vacancy concentration on the surface of the cathode material could

(29) Shiono, M.; Kobayashi, K.; Nguyen, T. L.; Hosoda, K.; Kato, T.; Ota, K.; Dokiya, M. *Solid State Ionics* **2004**, *170*, 1.

(30) Bouwmeester, H. J. M.; Den Otter, M. W.; Boukamp, B. A. J. *Solid State Electrochem.* **2004**, *8*, 599.

(31) Gao, J.; Liu, X.; Peng, D.; Meng, G. *Catal. Today* **2003**, *82*, 207.

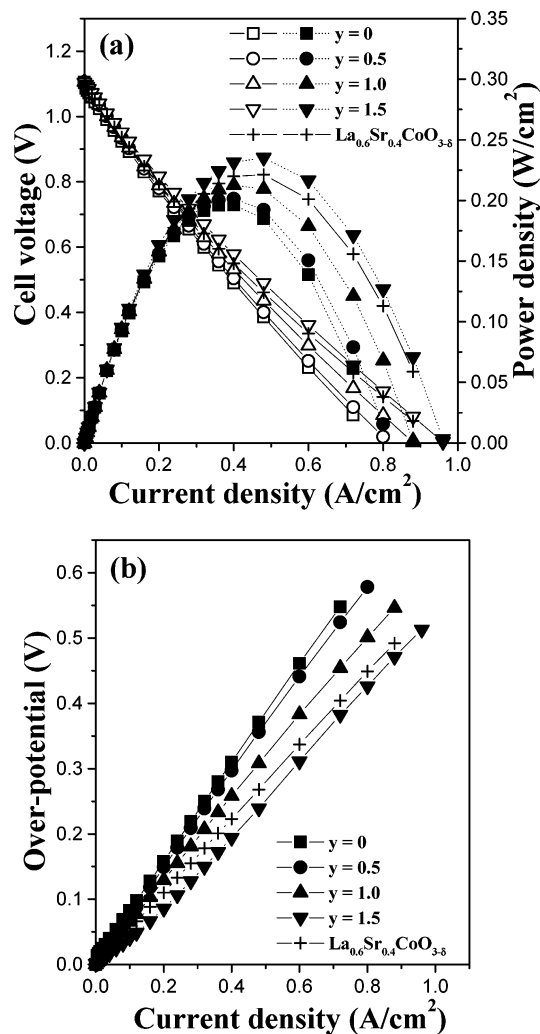


**Figure 9.** Comparison of (a) the  $I$ - $V$  curves (open symbols) and power densities (closed symbols) and (b) cathode overpotentials of the intergrowth  $\text{LaSr}_3\text{Fe}_{3-y}\text{Co}_y\text{O}_{10-\delta}$  ( $0 \leq y \leq 1.5$ ) cathodes with the GDC interlayer (fired at  $1100^\circ\text{C}$  for 3 h) at  $800^\circ\text{C}$ . For a comparison, the data for the perovskite  $\text{La}_{0.6}\text{Sr}_{0.4}\text{CoO}_{3-\delta}$  (fired at  $1000^\circ\text{C}$  for 3 h) are also shown.

improve the oxygen dissociation. Thus, an increase in the charge-transfer kinetics, oxide ion mobility, and surface exchange resulting from a substitution of  $\text{Co}^{3+}$  for  $\text{Fe}^{3+}$  leads to an increase in the electrochemical performance. More importantly, the  $\text{LaSr}_3\text{Fe}_{1.5}\text{Co}_{1.5}\text{O}_{10-\delta}$  cathodes with the GDC

interlayer show slightly better electrochemical performance than the perovskite  $\text{La}_{0.6}\text{Sr}_{0.4}\text{CoO}_{3-\delta}$  cathode. The lower TEC of the intergrowth  $\text{LaSr}_3\text{Fe}_{3-y}\text{Co}_y\text{O}_{10-\delta}$  cathodes ( $15.2$ – $20.4 \times 10^{-6} \text{ }^\circ\text{C}^{-1}$ ) compared to that of the perovskite  $\text{La}_{0.6}\text{Sr}_{0.4}\text{CoO}_{3-\delta}$  cathode ( $21.3 \times 10^{-6} \text{ }^\circ\text{C}^{-1}$ )<sup>32</sup> provides an added advantage with this new class of cathodes.

#### 4. Conclusions

With an aim to develop new cathode materials for intermediate temperature SOFCs, the mixed conducting  $\text{LaSr}_3\text{Fe}_{3-y}\text{Co}_y\text{O}_{10-\delta}$  ( $0 \leq y \leq 1.5$ ) oxides with a perovskite-related intergrowth structure have been investigated. The electrical conductivity of these intergrowth oxides are  $> 100 \text{ S/cm}$  above  $500^\circ\text{C}$ , which is acceptable to employ them as cathodes in SOFC, and the substitution of Co for Fe increases the conductivity because of an increase in the covalency of the (Fe,Co)-O bond. The TEC increases with increasing Co content because of the spin state transitions associated with the  $\text{Co}^{3+}$  ions and the formation of increasing degree of oxide ion vacancies. The porous GDC interlayer successfully prevents the unfavorable reaction between cathode and electrolyte, and the cathode with GDC interlayer exhibits good electrocatalytic activity. The electrochemical performance of the  $\text{LaSr}_3\text{Fe}_{3-y}\text{Co}_y\text{O}_{10-\delta}$  cathodes with a GDC interlayer increases with increasing Co content because of an increase in the electrical conductivity and oxide ion conduction. While the electrochemical performance is comparable to that of the well-known perovskite  $\text{La}_{0.6}\text{Sr}_{0.4}\text{CoO}_{3-\delta}$  cathode, this new class of  $\text{LaSr}_3\text{Fe}_{3-y}\text{Co}_y\text{O}_{10-\delta}$  intergrowth cathodes offers an important advantage of significantly lower TEC compared to that of the  $\text{La}_{0.6}\text{Sr}_{0.4}\text{CoO}_{3-\delta}$  perovskite. Additionally, the good structural stability of the intergrowth oxides without any phase transitions compared to the perovskite oxides may provide added benefits with respect to long-term stability.

**Acknowledgment.** This work was supported by the Welch Foundation Grant F-1254.

CM052645+

(32) Lee, K. T.; Manthiram, A. *J. Electrochem. Soc.*, in press.